

Reactive Organic Carbon Air Emissions from Mobile Sources in the United States

Benjamin N. Murphy^{1*}, Darrell Sonntag², Karl M. Seltzer³, Havalala O. T. Pye¹, Christine Allen⁴, Evan Murray⁵, Claudia Toro⁵, Drew R. Gentner⁶, Cheng Huang⁷, Shantanu Jathar⁸, Li Li⁶, Andrew A. May⁹, and Allen L. Robinson¹⁰

¹Center for Environmental Measurement and Modeling, US Environmental Protection Agency, Research Triangle Park, North Carolina 27711, United States

²Department of Civil and Construction Engineering, Brigham Young University, Provo, Utah 84602, United States

³Office of Air Quality Planning and Standards, US Environmental Protection Agency, Research Triangle Park, North Carolina 27711, United States

⁴General Dynamics Information Technology, 79 T.W. Alexander Drive, Research Triangle Park, NC 27709, United States

⁵Office of Transportation and Air Quality, US Environmental Protection Agency, Ann Arbor, Michigan 48105, United States

⁶Department of Chemical and Environmental Engineering, Yale University, New Haven, CT 06511, United States

⁷State Environmental Protection Key Laboratory of Cause and Prevention of Urban Air Pollution Complex, Shanghai Academy of Environmental Sciences, Shanghai, 200233, China

⁸Department of Mechanical Engineering, Colorado State University, Fort Collins, Colorado 80523, United States

⁹Department of Civil, Environmental and Geodetic Engineering, The Ohio State University, Columbus, Ohio 43210, United States

¹⁰Department of Mechanical Engineering, Carnegie Mellon University, Pittsburgh, Pennsylvania 15213, United States; Carnegie Mellon University Africa, BP 6150 Kigali, Rwanda

*Correspondence to: Benjamin N. Murphy (murphy.ben@epa.gov)

Abstract: Mobile sources are responsible for a substantial controllable portion of the reactive organic carbon (ROC) emitted to the atmosphere, especially in urban environments of the United States (U.S.). We update existing methods for calculating mobile source organic particle and vapor emissions in the U.S. with over a decade of laboratory data that parameterize the volatility and organic aerosol (OA) potential of emissions from onroad vehicles, nonroad engines, aircraft, marine vessels, and locomotives. We find that existing emission factor information from teflon filters combined with quartz filters collapses into simple relationships and can be used to reconstruct the complete volatility distribution of ROC emissions. This new approach consists of source-specific filter artifact corrections and state-of-the-science speciation including explicit intermediate volatility organic compounds (IVOCs), yielding the first bottom-up volatility-resolved inventory of U.S. mobile source emissions. Using the Community Multiscale Air Quality model, we estimate mobile sources account for 20-25% of the IVOC concentrations and 4.4-21.4% of ambient OA. The updated emissions and air quality model reduce biases in predicting fine-particle organic carbon in winter, spring, and autumn throughout the U.S. (4.3-11.3% reduction in normalized bias). We identify key uncertain parameters that align with current state-of-the-art research measurement challenges.

1. Introduction

Ambient particulate matter (PM) and ozone (O₃) have detrimental impacts on human health and the environment (U.S. Epa, 2019, 2020c; Pye et al., 2021) with disparate impacts across societal groups (Tessum et al., 2021). Non-methane organic gases (NMOG) are precursors to PM and O₃, and reducing NMOG could reduce criteria pollutants and their associated mortality throughout the United States (U.S.) (Pye et al., 2022a). Mobile source emissions continue to be a major contributor to modern anthropogenic NMOG emissions. In contrast to other NMOG sources such as vegetation, mobile emissions have been reduced through successful regulatory policy and the introduction of cleaner engine and control technologies (Lurmann et al., 2015; Gentner et al., 2017; Winkler et al., 2018; Bessagnet et al.,

45 2022). Yet, effective management of urban and regional air quality still depends on accurate and detailed
46 characterization of the carbon-containing compounds emitted by mobile sources.

47 Fossil-fuel combustion emissions comprise thousands of organic compounds with widely varying volatility,
48 depending on source type (Drozd et al., 2018; Lu et al., 2018). The lowest volatility compounds are emitted principally
49 in the particle phase and are typically classified as primary organic aerosol (POA). Conventionally this portion of
50 emissions is sampled using filters which are weighed or processed off-line with thermal-optical techniques, solvent
51 extraction, and other methodologies (Chow et al., 1993; Birch and Cary, 1996; U.S. Epa, 2022c). The highest volatility
52 NMOGs are emitted in the gas-phase and enhance O₃ formation when oxidized in the atmosphere, a process that also
53 enhances PM mass via secondary organic aerosol (SOA) formation. U. S. EPA emission tools like the MOTO Vehicle
54 Emission Simulator (MOVES) (U.S. Epa, 2020b) and the SPECIATE database (U.S. Epa, 2020a) provide emission
55 estimates and speciation for POA (assumed to be nonvolatile) and NMOGs. The ‘Conventional’ path in Fig. 1 depicts
56 this process.

57 However, laboratory and field measurement campaigns have demonstrated that much of the mobile source POA is
58 subject to gas-particle partitioning and filter sampling artifacts. These artifacts may bias the interpretation of filter-
59 based measurements by yielding higher POA emission factors due to the presence of these adsorbed vapors (Turpin
60 et al., 1994; Robinson et al., 2010; Bessagnet et al., 2022). These compounds principally include (Table 1) semivolatile
61 organic compounds (SVOCs) and intermediate volatility organic compounds (IVOCs)(May et al., 2013b, a).
62 Accurately representing SVOCs and IVOCs is important because they are SOA precursors and are underestimated in
63 contemporary models and emission databases (Gentner et al., 2012; Tkacik et al., 2012; Zhao et al., 2014; Zhao et al.,
64 2015, 2016b).

65 Some air quality models (AQMs) have incorporated SVOCs and IVOCs by scaling these emissions to sector-wide
66 POA or NMOG inputs during a data pre-processing step or the AQM runtime (Murphy and Pandis, 2009; Shrivastava
67 et al., 2011; Ahmadov et al., 2012; Bergström et al., 2012; Koo et al., 2014; Woody et al., 2015; Zhao et al., 2016a;
68 Woody et al., 2016; Jathar et al., 2017b; Murphy et al., 2017). However, these approaches rely on broad application
69 of assumptions that may not be appropriate for specific source types since sampling artifacts will bias low-emitting
70 and high-emitting sources differently (Robinson et al., 2010). As emissions from individual combustion sources are
71 continually reduced in response to tightening regulations, accounting for these potential biases becomes important.
72 Manavi and Pandis (2022) and Sarica et al. (2023) implemented emission factors and speciation of SVOCs and IVOCs
73 specific for mobile sources in Europe, while Morino et al. (2022) explored revisions to stationary source organic
74 emissions in Japan. Chang et al. (2022) implemented a more detailed bottom-up inventory of organic emissions across
75 all sectors in China with emission factors specified at the volatility bin level rather than for bulk PM and NMOG.
76 Additional bottom-up approaches are needed that revise emission factors and speciation profiles for all relevant
77 individual source types and regions.

78 This paper documents the transition of U. S. EPA mobile emission tools from the conventional paradigm that considers
79 operationally defined particulate organic matter (OM) and NMOG emission factors and speciation to one that
80 accommodates the full complexity of atmospheric carbon-containing trace pollutants. To accomplish this, we consider

81 total Reactive Organic Carbon (ROC), defined by Saffedienne et al. (2017) and Heald and Kroll (2020) as all reactive
82 organic compound mass across gas and particle phases excluding methane. We catalogue updates to 51 diverse mobile
83 source categories across multiple categories and engine, fuel, and control types. Further, we demonstrate procedures
84 for integrating existing inventory emission factors with state-of-the-art chemical composition measurements, pointing
85 out where critical uncertainties could be further resolved in the future. Finally, we document the impact the updates
86 have on source-specific and sector-wide emissions as well as regional-scale pollutant formation and transport
87 predicted by an updated version (2020) of the Community Multiscale Air Quality (CMAQ) regional-scale AQM.

88 **2. Materials and Methods**

89 **2.1 Mobile Emission Modeling**

90 To develop the new framework and estimate potential impacts from speciation updates, we used existing estimates for
91 2016 annual mobile emissions for the contiguous U.S. We considered five categories including onroad, nonroad, air,
92 rail, and marine. The MOVES3 model predicted emissions for onroad and nonroad sources using county-level fleet
93 properties and activity data. The dominant U.S. onroad vehicle sources were light-duty gasoline cars and trucks and
94 heavy-duty diesel trucks. Nonroad emission sources included construction, agricultural, and lawn equipment as well
95 as nonroad recreational vehicles. The Aviation Environmental Design Tool (AEDT), maintained by the Federal
96 Aviation Administration, predicted landing, taxi, and take-off emissions for aircraft and emissions from ground
97 support equipment (FAA, 2022). Rail emissions were calculated using confidential line-haul activity data that were
98 summarized at the county-level, while rail-yard emissions were based on supply fuel use and yard switcher counts
99 provided by companies (U.S. Epa, 2022b). Marine emissions included both port and underway conditions for large,
100 generally international ships, vessels, and smaller boats operating near shore (U.S. Epa, 2022b). The MOVES3 model
101 predicted emissions from recreational boats as part of the nonroad recreational equipment category.

102 We also collected national total annual fuel usage data for each source from the models to calculate an effective fuel-
103 based OM emission factor (see section S1). These effective emission factors ranged from 1-20 mg (kg-fuel)⁻¹ for the
104 newest gasoline, diesel, and compressed natural gas (CNG) vehicles to over 6000 mg (kg-fuel)⁻¹ for nonroad gasoline
105 two-stroke engines. In the process of reviewing each mobile source OM emission rate, we discovered and corrected
106 several minor errors and limitations to compressed natural gas sources and uncontrolled nonroad diesel exhaust (see
107 section S2).

108 **2.2 Reactive Organic Carbon (ROC)**

109 To accurately simulate the behavior of mobile emissions, we considered total ROC, which includes organic carbon
110 (OC) and non-carbon mass from the most volatile compounds like ethane and formaldehyde to chemically complex,
111 high molecular weight, low-volatility compounds (e.g. oligomers) (Heald and Kroll, 2020). Conventional metrics for
112 reporting OM and NMOG are operationally defined based on measurement methods and conditions; therefore, they
113 are difficult to compare across tests and among other ROC sources. Furthermore, uncertainties are introduced when
114 they are speciated with profiles measured at different conditions. To improve standardization, we introduced two new
115 metrics: CROC (condensable reactive organic carbon) and GROC (gaseous reactive organic carbon). CROC was
116 defined as compounds with saturation concentration (C^*) less than 320 $\mu\text{g m}^{-3}$ (Table 1), with this boundary

117 corresponding to *n*-alkanes with 20 ± 1 carbon atoms. CROC included SVOCs ($0.32 < C^* \leq 320 \mu\text{g m}^{-3}$) and low
118 volatility organic compounds (LVOCs; $C^* \leq 0.32 \mu\text{g m}^{-3}$). Whereas, GROC was defined as the sum of compounds
119 with C^* greater than $320 \mu\text{g m}^{-3}$ corresponding to IVOCs ($320 < C^* \leq 3.2 \times 10^6 \mu\text{g m}^{-3}$) and volatile organic compounds
120 (VOCs; $C^* > 3.2 \times 10^6 \mu\text{g m}^{-3}$) (Donahue et al., 2009; Murphy et al., 2014). CROC and GROC aligned with well-
121 known categories in the volatility basis set (VBS) space, so they could be applied straight-forwardly to speciation
122 profiles in recent literature containing both explicit compounds and lumped groups.

123 We applied a two-step methodology to process gas- and particle-phase emissions ('ROC' path in Fig. 1). First, we
124 estimated total GROC and CROC emissions from existing NMOG and OM emission factors, respectively, while
125 considering measurement uncertainties like sampling setup losses (e.g., tubing) and filter artifacts. We then speciated
126 GROC and CROC using state-of-the-science profiles. For GROC, these included explicit IVOC compounds, where
127 available, and lumped IVOC groups distinguished by their saturation concentration and functionality. The
128 methodology for processing CROC emissions similarly used volatility profiles from recent literature.

129 **2.2.1 GROC Emissions and Speciation**

130 Total NMOG emissions are measured from mobile emissions by combining total hydrocarbons (THC) with carbonyl
131 compounds and subtracting methane (see section S3) (Kishan et al., 2006; May et al., 2014). Lu et al. (2018) compiled
132 measurements for onroad vehicles, nonroad equipment, and an aircraft turbine engine. That study concluded that
133 methods using heated sampling and a heated flame-ionization detector (FID) captured both IVOCs and VOCs, but
134 that speciation methods like canister or tedlar bag sampling analyzed with gas-chromatography-FID missed essentially
135 all IVOCs due to wall losses to the sampling materials. Assuming that NMOG emission rates are based on heated FID
136 sampling, we set GROC emission rates equal to total NMOG emission rates across all sources, and we speciated
137 GROC emissions using profiles that include VOCs and IVOCs.

138 Many studies have reported speciated organic gases normalized to total IVOC or VOC (Lu et al., 2018; Jathar et al.,
139 2017a; Zhao et al., 2015, 2016b; Huang et al., 2018; Drozd et al., 2018). A key parameter used to integrate these data
140 is the IVOC/NMOG ratio (see section S4), which ranges from ~4.6% for gasoline vehicle cold start exhaust to 67%
141 for marine residual oil. Gasoline fuel evaporation profiles of GROC were assumed to be the same as NMOG since
142 IVOCs are not expected to contribute substantially to those emissions (Gentner et al., 2012). The profile for whole
143 diesel fuel evaporation was updated to be consistent with fuel characterization in Gentner et al. (2012) (see Section
144 S1c). SPECIATEv5.1 contains thousands of explicit species and many mixtures of compounds (e.g., oils, unspeciated
145 terpenes, etc.) reported by previous studies. Recent studies have constrained the unknown portion of IVOCs and VOCs
146 with lumped groups resolved by volatility and often by structure/functionality features (e.g., branched, cyclic,
147 oxygenated, etc.). We leveraged the representative compound structures in SPECIATE developed by Pye et al. (2022b)
148 to classify these emissions by functional groups, and their subsequent atmospheric chemistry. Table S2 summarizes
149 the new IVOC profiles. Species-based ozone and OA potential were calculated for each emission source using
150 relationships from Seltzer et al., (2021) which were expanded by Pye et al. (2022b)

151 2.2.2 CROC Emissions and Speciation

152 We estimated effective OM emission factors using the MOVES-predicted national total OM emissions normalized to
153 the total fuel usage for each source (see section S1). The MOVES model relied on conventional measurements of total
154 PM emissions sampled and weighed on Teflon filters. The profiles available in the SPECIATE database, meanwhile,
155 provide the weight percent of OC measured by thermal optical techniques from samples collected on quartz filters
156 (U.S. Epa, 2022c) normalized by coincident bulk PM measurements from the Teflon filter (see section S5).
157 SPECIATE profiles also include a source-dependent OM/OC factor to adjust for non-carbon organic mass (i.e.
158 hydrogen, oxygen), which represents OM once added to OC (Table S1a) (Reff et al., 2009; Simon et al., 2011).
159 Previous studies have demonstrated that OM emission factors vary with changing temperature and OM loading
160 (Lipsky and Robinson, 2006; Robinson et al., 2010; May et al., 2013a, b; Jathar et al., 2020). AQMs that have taken
161 this behavior into account typically distributed OM emissions among volatility bins using reference distributions. May
162 et al. (2013a, b) constrained parameters for calculating volatility-resolved emissions assuming OC is measured on a
163 quartz filter. Although this approach performs well for average cases, it is less accurate when applied to sources that
164 are low or high emitting, for which absorptive partitioning biases are more substantial (Fig. 2). For an exceedingly
165 low-emitting source (low OM loading), SVOC emissions that would normally partition to the particle phase under
166 ambient conditions could go undetected as they pass through the filter.

167 Additionally, reported OM emissions are sometimes artifact-corrected using a secondary quartz filter behind the
168 Teflon filter sample, which allows for adsorbed SVOCs and IVOCs to be neglected. Because these corrections are not
169 uniformly applied across all studies, May et al. (2013a, b) reported reference volatility profiles assuming OM emission
170 factors had not been adsorptive-artifact corrected. Yet this is not always applicable for the emission rates informing
171 MOVES and must be resolved at the source level based on the underlying emission data. To address both adsorptive
172 and absorptive partitioning biases, we applied CROC/OM parameterizations developed from detailed measurement
173 data and informed by filter-based OM emission factors (see section S6) (May et al., 2013a, b; Huang et al., 2018;
174 Jathar et al., 2020). The method accounted for filter artifact corrections by adding missing SVOC emissions for low
175 OM-loading tests and neglecting IVOCs and higher-volatility SVOCs that would be captured on the front filter during
176 high OM-loading tests. The CROC/OM parameterization for onroad gasoline was based on data from 64 vehicles and
177 so was more robust than the parameterization for onroad heavy-duty diesel with particulate filters (DPF), which was
178 based on 3 vehicles (Section S7), or the aircraft engine parameterization, which was based on one sample. These
179 datasets showed that it was possible to represent the relationship between OM emission factor and CROC emission
180 factor without explicitly considering variations in temperature and OM concentration. This simplified approach was
181 limited to mobile sources because temperature was tightly controlled by test method requirements (i.e., 47 °C). We
182 used temperature to calculate c^* of partitioning components and then calculate total CROC (e.g., Fig. S4). Because the
183 resulting CROC emission factor was highly correlated with OM emission factor, the simplified functions associating
184 them accounted for variations due to the underlying volatility distribution and increases in concentration with emission
185 factor. More work is needed to better constrain the CROC/OM parameters.

186 The impact of this new approach for translating inventory OM emissions is shown in Fig. 2. We used the onroad
187 gasoline light-duty cold start volatility profile in Table S5 to estimate the effective ambient organic aerosol emission

188 factor at 298 K and C_{OA} equal to $10 \mu\text{g m}^{-3}$ given a filter-based OM emission factor in mg kg^{-1} fuel. Also shown are
189 trends using parameters reported by Robinson et al (2007) and Lu et al. (2020), which have been used in contemporary
190 air quality models. The filter-based OM emission factor (EF_{OM}) was multiplied by the volatility distribution, and VBS
191 partitioning theory (Eq. 1) was used to calculate the effective ambient OA emission factor ($EF_{OM,Amb}$):

$$192 \quad EF_{OM,Amb} = EF_{OM} \sum_{i=1}^{n_{tot}} \frac{\alpha_i}{1 + C_i^*/10} \quad (1)$$

193 Where n_{tot} was the number of volatility parameters in the vector α and ambient conditions were defined to be 298 K
194 and $10 \mu\text{g m}^{-3}$. The ‘Lu et al.’ and ‘Robinson et al.’ trends are directly proportional to the nonvolatile emission factor
195 because they do not consider nonlinear dependence on the filter-based OM emission factor. Meanwhile, the ROC
196 approach enhances emissions at low emission factors (to correct for SVOC breakthrough) and reduces them at high
197 emission factors (to remove IVOCs partitioning to the filter). Also shown in Fig. 2 are representative filter-based OM
198 emission factors for PreTier 2, Tier 2 (2001-2004), and Tier 2 (2004+) vehicles, which together exhibit emissions
199 reductions with newer standards. For the older vehicles, the ‘Lu et al.’ and ‘Robinson et al.’ approaches give similar
200 estimates for effective ambient OM as the new approach, but as emission factors decrease, those methods may
201 overpredict evaporation and underpredict the particle emission factors. At the lowest OM emission factors, even using
202 the nonvolatile approach may underpredict effective ambient OA emission factors because significant SVOCs could
203 have broken through the filter and should be considered for ambient partitioning.

204 We did not adjust GROC emissions in response to CROC/OM conversion, but the sum of total ROC emissions for
205 each source did not change substantially from the sum of NMOG and OM (Fig. S22). We updated existing SPECIATE
206 profiles with volatility distributions of LVOCs and SVOCs normalized to CROC (Table S5a). Because data on the
207 functionality of these low volatility emissions is lacking, we assumed they share similar chemical properties (i.e.
208 reactivity) to linear alkanes as a proxy for more complex mixtures of aliphatics and other compounds.

209 **2.3 Air Quality Model Configuration**

210 We used an updated version of the Community Multiscale Air Quality (CMAQ) model v5.3.2 to quantify the impact
211 of the new mobile emissions on regional-scale air quality (U.S. Epa, 2021; Appel et al., 2021). Hourly ambient air
212 concentrations of OA and O_3 were simulated for the entire year 2017 at 12 km horizontal resolution with inputs from
213 EPA’s air QUALity TimE Series (EQUATES) project (U.S. Epa, 2022a; Foley et al., 2023). Meteorology was
214 simulated with WRFv4.1.1. The Biogenic Emission Inventory System (BEIS) predicted biogenic gas emissions online
215 in CMAQv5.3.2. Gas- and aerosol-phase chemistry were modeled with the Carbon Bond 6 mechanism (CB6r3_AE7)
216 with updates for production of SOA from mobile IVOCs implemented by Lu et al. (2020) Anthropogenic emissions
217 are described in the US EPA 2017 emission platform technical science document and EQUATES documentation (U.S.
218 Epa, 2022b, a). Mobile emissions for 2017 were recalculated in order to update speciation and apply both
219 IVOC/NMOG and CROC/OM adjustments. The ‘CMAQ-ROC’ simulation implemented all revisions to mobile
220 elemental carbon (EC) speciation described in section S2 and the methods described in sections 2.2.1 and 2.2.2. The
221 EC speciation updates resulted in substantial changes to nonroad diesel, aircraft, marine and rail source (Table S9).
222 Because MOVES used source- and species-specific emission rates for HAPs rather than relying on generic speciation

223 of NMOG, ROC updates for HAPs were not propagated to the air quality model simulations, although Fig. S25 shows
224 potential changes to national-scale HAP emissions from updates to VOC speciation. Volatile chemical product (VCP)
225 emissions were simulated for 2017 with the VCPy tool (Seltzer et al., 2021). Nonoxygenated and oxygenated IVOC
226 emissions from VCPs were represented with the IVOC chemistry from Lu et al. (2020), which resulted in an average
227 SOA yield of approximately 30% at ambient conditions across all IVOCs. However, Pennington et al. (2021) found
228 the oxygenated IVOC SOA yield to be 6.28%, though this yield warrants re-evaluation with better speciation and yield
229 data given the diverse mix of oxygenated IVOCs with varying molecule functionalities that can influence SOA
230 production (Humes et al., 2022). Based on available information, we reduced the CMAQ-predicted VCP SOA
231 concentrations by 33.8% to account for the overrepresentation of SOA from VCP oxygenated IVOCs (see section S7).

232 We assessed model performance for O₃ and OC during the 2017 model year with daily-averaged measurements at
233 routine monitoring sites. We also performed a separate CMAQ simulation for comparison that is consistent with the
234 EQUATES project, which assumed the speciation of OM emissions from all sources were consistent with the volatility
235 distribution of a small diesel generator (Robinson et al., 2007). This ‘EQUATES’ simulation also utilized the
236 simplified potential-combustion SOA (pcSOA) approach used in publicly available versions of CMAQ (Murphy et
237 al., 2017). The CMAQ-ROC simulation neglected pcSOA since the role of mobile and VCP IVOC SOA formation
238 were explicitly accounted for. Finally, we analyzed two sensitivity simulations with mobile and VCP SOA precursors
239 each set to zero to quantify direct sector contributions to total OA. This approach did not account for the contributions
240 these sectors make to the atmospheric oxidant capacity through emissions of low molecular weight VOCs and nitrogen
241 oxides.

242 **3. Results and Discussion**

243 **3.1 Volatility-Resolved Mobile Source ROC Emissions**

244 Using the 2016 annual predictions from MOVES and the other mobile emission models processed and speciated with
245 the ‘ROC’ approach, we explore for the first time a complete bottom-up inventory of organic carbon emissions from
246 mobile sources in the U.S. Figure 1 shows the results of the ROC and Conventional approaches for one example
247 source, onroad heavy-duty diesel equipped with particulate filters. Non-organic particulate matter species such as ions
248 and other PM are equivalent in both approaches. Nonvolatile OM emissions in the Conventional approach are
249 distributed in the ROC approach to a range of SVOCs and IVOCs, which are predominantly alkanes and branched
250 compounds for diesel sources. The magnitude of emission factors for compounds in the VOC volatility range from
251 onroad diesel sources are reduced by 47.8% due to the introduction of IVOCs (IVOC/GROC = 52.2%), and the
252 distribution of VOC functionality is changed substantially due to adoption of VOC speciation profiles from Lu et al.
253 (2018). Unknown ROC mass is also reduced from 7% of total emissions to 0.7% after introducing IVOCs. Emission
254 factors vary by orders of magnitude across mobile sources, motivating careful accounting of sampling biases (Figs.
255 S18-S21), which requires the ROC approach in the emission modeling workflow to be complex and involve multiple
256 tools and intermediate steps (Fig. S1).

257 Figure 3 shows the predicted contributions of source types and functional groups across the volatility spectrum for
258 2016 ROC inventory. The VOC emissions are roughly evenly distributed between onroad and nonroad sources (1130

259 and 1045 kt yr⁻¹, respectively), IVOCs are weighted towards onroad (62%), and CROC (i.e. SVOCs and larger
260 compounds) is roughly split among onroad, nonroad, and others. Tailpipe (i.e. exhaust) emissions while running
261 represent the majority across all volatility categories (56% of total ROC), although evaporative sources are important
262 in the VOC range (38%), and similar to prior estimates (Gentner et al., 2009). It could be counter-intuitive, given
263 laboratory data on start and idle emission factors, that the start/idle operating mode does not contribute more to total
264 ROC emissions. This result could be due in part to substantially more time spent by sources in the running mode
265 during normal operation, but it could also be partly due to MOVES neglecting start modes for nonroad sources. Drozd
266 et al. (2018) found that cold start IVOC fuel-based emission factors are about 6 times larger than those from hot-
267 running-start emissions for newer vehicles, which is consistent with the post Tier 2 gasoline vehicles in this work. For
268 older vehicles though, the ROC inventory predicts greater IVOC emissions factors for hot-running modes than cold-
269 start for older vehicles (Table S1a and Table 2). Further research is needed to constrain NMOG emission factors and
270 IVOC/NMOG ratios for older (pre-2004) vehicles that are expected to have contributed approximately 72% of onroad
271 gasoline ROC emissions during 2017 (see Fig. S24 and Table S1a).

272 Emissions from gasoline-fueled sources dominate the VOC range in Fig. 3, but diesel-fueled sources, of which there
273 are far fewer in the U.S. dominate the IVOC range. Whereas, sources using both fuels are important for CROC
274 emissions. Mobile source VOCs comprise many functionalities, and aromatics make a substantial contribution. The
275 higher volatility IVOCs have mass associated with aromatics from gasoline sources, but cyclic hydrocarbon
276 compounds contribute to IVOCs across all volatilities, a feature reported by Zhao et al. (2015) We currently lack data
277 to specify CROC functionality across all mobile categories, so we have labeled them alkane-like based on observations
278 of motor vehicle POA emissions (Worton et al., 2014). Improved CROC speciation is needed, especially given the
279 importance of functionality to SOA formation (Lim and Ziemann, 2009; Yee et al., 2013).

280 **3.2 Impact of Filter Artifacts**

281 Transitioning from the Conventional approach to the ROC approach has implications for near-source particle
282 concentrations and prompt SOA production. Figure 4 shows the contributions of mobile categories with results using
283 approaches from previous work (Murphy et al., 2017; Lu et al., 2020). The Conventional approach assumes all OM
284 stays in the particle phase, which has been shown to lead to poor AQM performance (Murphy et al., 2017). The
285 ‘Robinson et al.’ case, which is consistent with CMAQv5.3.2, applies the volatility distribution for a small nonroad
286 diesel engine, where half the OM mass is assumed to be IVOCs adsorbed to filters and is thus volatilized. As seen in
287 Fig. 4, only 25% of the OM persists in the particle after evaporation in the ‘Robinson et al.’ approach. Lu et al. (2020)
288 applied gasoline and diesel-specific volatility profiles parameterized for emissions from in-use vehicles to the entire
289 mobile category, leading to less evaporation of OM than the ‘Robinson et al.’ approach. Lu et al. (2020) also applied
290 a conversion factor of 1.4 to all mobile gasoline-fueled sources to account for missing SVOCs.

291 In the ROC approach here, we apply source-specific adjustment factors (Table S6) and volatility profiles (Table S5)
292 and find similar results for onroad gasoline and nonroad diesel compared to Lu et al. (2020). However, onroad diesel
293 CROC emissions are increased by 60% relative to the CROC emissions from the ‘Lu et al.’ approach, driven by the
294 inclusion of missing SVOCs from clean test conditions for diesel engines with DPFs. Conventional OM emissions

295 from nonroad sources are greater than those from onroad for both gasoline- and diesel-fueled sources. Nonroad
296 gasoline emissions reduced by 36% relative to 'Lu et al.' where emission factors are large, and CROC/OM is much
297 less than 1.0 (Table S6), indicating the presence of IVOCs on the filter. Predicted conventional OM emissions from
298 air, rail, and marine sources are also important, and CROC emissions are slightly larger than OM. Across the mobile
299 sector, total CROC emissions increased by 12% relative to OM, and 42% of the CROC emissions are predicted to be
300 in the particle phase at 298 K and 10 $\mu\text{g m}^{-3}$ organic aerosol (OA) loading.

301 **3.3 National-Scale Impact on PM, O₃ and HAPs**

302 When aggregated across all mobile sources, total ROC emissions are nearly identical between the Conventional
303 approach and ROC approach (Fig. 5). Total IVOC emissions represent only 10.2% of total GROC due to the
304 substantial role of VOCs from gasoline sources to ROC emissions in the U.S. The spatial distribution of IVOC and
305 CROC emissions highlight the key role of cities, highways, and shipping lanes (Fig. S26). We calculate the OA
306 potential as the sum of particle-phase mass (calculated at 298 K and 10 $\mu\text{g m}^{-3}$) for each species and the SOA yield of
307 the vapor-phase component of each species. Mobile source OA potential has contributions from all ROC volatility
308 classes with 6.8% from LVOCs, 25.4% from SVOCs, 19.1% from IVOCs, and 48.7% from VOCs (Fig. 5). The
309 estimated VOC OA potential is mainly driven by adjusted yields of aromatic VOCs, which are enhanced over previous
310 work due to corrections for vapor wall-losses of single-ring aromatic yields (Zhang et al., 2014). These metrics
311 possibly reflect an upper bound on VOC and IVOC contribution as they apply SOA yields to the precursor emission
312 without consideration of reaction rates, timescales, or competitive losses of precursors and intermediates to deposition.
313 Potential OA relative contributions from air, marine, and rail (12%) and onroad diesel (16%) sources play a larger
314 role in OA potential when emissions are estimated with the ROC approach, while nonroad gasoline and diesel (38%)
315 and onroad gasoline potential OA (34%) decrease (Fig. 6). While aromatic species dominate OA potential in the VOC
316 precursor range, in the IVOC range OA potential has larger contributions from cyclic alkane compounds from onroad
317 diesel sources (Fig. S23). In the LVOC range and below, the ROC approach assumes only alkane-like species;
318 improvements to the SPECIATE database and emissions modeling tools will support increased detail on compound
319 functionality when provided by future studies.

320 VOCs account for 97% of the ozone potential approximated by maximum incremental reactivity (MIR), and the total
321 ozone potential decreases by 8.9% due to the shift in mass from VOC to IVOC. The national-scale source distribution
322 of O₃ potential changes little between the Conventional and ROC approaches (Fig. 6). Ozone potential is dominated
323 by onroad and nonroad gasoline sources in the highest ROC volatility bins, driven by alkane, aromatic, and oxygenated
324 species, as expected (Fig. S23). Among onroad light duty gasoline vehicles, 72% of ROC emissions, 68% of O₃
325 potential, and 79% of OA potential are predicted to come from pre-Tier 2 vehicles, while these vehicles account for
326 19% of the fuel used in 2017 (Fig. S25). Heavy-duty diesel vehicles without particulate filters or selective catalytic
327 reduction systems contribute 87% of ROC emissions, 85% of O₃ potential, and 91% of OA potential while using 31%
328 of the fuel for the heavy-duty diesel onroad category.

329 National-scale HAP emissions changed substantially with updates in VOC speciation and introduction of IVOCs with
330 many species decreasing by nearly 20% or more including toluene (-19%), hexane (-22%), 1,3-butadiene (-34%), and

331 ethyl benzene (-29%) and others increasing substantially including formaldehyde (+22%), acrolein (+20%), and
332 acetaldehyde (+19%) (Fig. S25). These results emphasize the need for more research on HAP emission factors, but
333 we keep them constant for the CMAQ simulations to focus on OA and O₃ changes.

334 **3.4 Air quality model results**

335 Mobile ROC emissions were generated for the year 2017 to be comparable with the EQUATES 2017 emission inputs.
336 Differences between the EQUATES mobile inputs and those for the CMAQ-ROC simulation (Table S9) are consistent
337 with the changes in the 2016 emissions results depicted in Fig. 4. The CMAQ-ROC simulation predicts lower OC
338 concentrations throughout the domain due to elimination of pcSOA. CMAQ-ROC predictions compared well against
339 both O₃ and OC measurements at Air Quality System (AQS) sites in 2017 (Figs. S28, S29 and Table S10). Normalized
340 mean biases for OC improved (in absolute terms and on average) by 11.3% in spring, 4.3% in autumn, and 7.6% in
341 winter. In summer, the OC underprediction increased by 12%. Overprediction in the northeast, Ohio Valley, Upper
342 Midwest, and northwest in winter is consistent with timing and geography of residential wood combustion emissions,
343 which may be overrepresented in both simulations. Root mean square error and correlation coefficient differences
344 between the EQUATES and CMAQ-ROC simulations are small. CMAQ predicts both the annual mean and variability
345 of OC concentrations well at selected U.S. cities (Fig. S34, S35), with the exception of New York City where the
346 model overpredicted OC by more than a factor of 2.

347 The predicted annual population-weighted average OA attributable to mobile sources is 0.26 μg m⁻³, or 9% of the OA
348 from all anthropogenic and biogenic sources. Mobile source contributions to POA and SOA are similar on average,
349 with apparent spatial differences (Fig. 7). Average total mobile source OA appears stable between winter and summer
350 seasons (Fig. S30), and this is a result of trade-offs between higher POA concentrations in winter and higher SOA in
351 summer (Figs. S31, S32). In rural areas, model-predicted mobile OA contributions asymptote at 4.5% of total OA,
352 and in some urban areas they can exceed 23% (annual averages; Fig. S33). The ratio of SOA to OA is equal to 70%
353 in rural areas and decreases with increasing population to 20-40%. Diurnal profiles at select cities indicate SOA
354 formation peaks at noon in Los Angeles, Denver, Chicago and New York, but that feature is not reproduced on average
355 at Houston and Raleigh (Figs S34, S35).

356 CMAQ-ROC mobile and VCP IVOC concentrations are enhanced in urban areas with minimal seasonal differences
357 predicted (Figs. S36, S37). Mobile sources are predicted to contribute 20-25% to total IVOCs depending on location
358 and time of year, while VCP sources contribute 59-66% (Fig. S36), although IVOCs from other sources are
359 underrepresented. The composition of ambient IVOCs predicted by CMAQ-ROC and the speciation of IVOC
360 emissions from mobile and VCP emissions are consistent with results from Zhao et al. (Fig. S38). Since ambient
361 IVOC concentration measurements for 2017 are lacking, we extrapolated concentrations to the CalNex campaign in
362 2010 and find acceptable agreement with campaign-average hydrocarbon and oxygenated IVOC observations (section
363 S8, Fig. S39a,b). Extrapolation of CMAQ-ROC SOA to 2010 underpredicts mean CalNex SOA observations by 46%
364 (Fig. S39c,d). Potential explanations include underestimated emissions from other sources (e.g. cooking),
365 mischaracterized chemical processing (e.g. SOA yields), or errors in modeling regional pollution in Southern
366 California (Lu et al., 2020).

367 The U.S. annual GROC emission rate for mobile (2.49 Tg yr^{-1}) is 20% less than that of VCPs (3.09 Tg yr^{-1}), but the
368 mobile IVOC emissions (0.25 Tg yr^{-1}) are only one third those of VCPs (0.77 Tg yr^{-1}). Gas-phase oxidation is
369 responsible for less than half (42% and 44%) of the loss of mobile and VCP SOA-forming GROC, but 88-90% of the
370 IVOC loss (Fig. 8). The annual production and loss of total OA from mobile and VCPs is similar, and loss is distributed
371 evenly across deposition processes and transport out of the model domain. The annual rate of OA production (emission
372 plus chemical production) estimated by CMAQ and normalized to total ROC emissions (i.e. the sum of NMOG plus
373 conventional OM) is $0.16 \text{ g OA (g ROC)}^{-1}$, which is approximately equal to that estimated from the data in Fig. 5. This
374 agreement is surprising considering that the latter calculation does not account for variations in OA partitioning, NO_x
375 effects on SOA yields, or competitive losses from wet scavenging and dry deposition. Seasonal trends for OA, SOA
376 and POA production rates and ambient concentrations normalized to OM and NMOG emissions are tabulated in Table
377 S11 and discussed in section S9. These data may inform simple (e.g. screening) models of the impact of anthropogenic
378 emissions on human exposure.

379 4. Conclusions

380 This study implements a detailed source- and species-level procedure for converting conventional OM and NMOG
381 mobile emissions to metrics compatible with the most recent science and speciation developed for atmospheric ROC.
382 Although many AQMs have implemented online or pre-processing emission adjustments to account for these
383 phenomena, (Koo et al., 2014; Murphy et al., 2017) the procedure should be embedded within emission models and
384 databases for several reasons. Most importantly, this detailed approach considers a more diverse population of sources
385 of different ages, fuels, and control technologies that are typically averaged together before they are passed to the
386 AQM. Additionally, the new procedure enables near-explicit speciation of each emission source before mapping to
387 model species used in a particular chemical mechanism. Having a detailed speciation of major emission sources is
388 critical for assessing and revising chemical mechanisms (Pye et al., 2022b). Finally, operationalizing conversions from
389 OM to CROC and NMOG to GROC alleviates AQM users from the burden of interrogating their emissions files to
390 determine whether complex scaling operations are needed. From the broader perspective of facilitating transfer of
391 knowledge between the scientific and regulatory communities, the SPECIATE database is now capable of ingesting
392 speciation profiles with factors aligned with the most recent research studies and has enhanced flexibility to
393 accommodate future updates. Nonetheless, for model applications seeking to scale legacy emission inputs, we provide
394 updated factors normalized to several levels of source aggregation in Table S12 and discuss the uncertainty introduced
395 with this approach in section S10.

396 The 2016 ROC emissions suggest slight decreases to total O_3 formation due to reappportionment of VOC to IVOC in
397 this approach, but 2017 CMAQ-ROC predictions do not meaningfully change when evaluated at AQS sites.
398 Meanwhile, mobile SVOC and IVOC emissions enhance OA formation by an additional 79 kt yr^{-1} compared to
399 estimates from the EQUATES configuration (319 kt yr^{-1}). Gaps between total OA measurements and CMAQ-ROC
400 predictions will be addressed through improved modeling of other sources of ROC (e.g., VCPs, wildfires, residential
401 wood combustion, and cooking). Within the mobile sector, results indicate substantial contributions from onroad
402 (46%) and nonroad (41%) gasoline and somewhat less from onroad (5%) and nonroad (3%) diesel air, marine, and

403 rail sources (4.7%; Fig. 6). The vast majority of ROC emissions and impacts are attributable to older (pre-Tier 2 light
404 duty gasoline and non-DPF heavy duty diesel) vehicles and nonroad gasoline engines. Onroad pollution will continue
405 to decrease as these vehicles are phased out, increasing the importance of other mobile source categories and other
406 sources.

407 This study suggests several specific uncertainties pertaining to mobile source emissions need further laboratory and
408 field investigation. Developing complete ROC volatility distributions for specific source classes and control types is
409 critical, especially within the nonroad category where fewer experimental data were available for this study. The
410 CROC/OM factors are uncertain across all mobile sources. Ideally, IVOC and CROC emissions should be sampled
411 by a filter and a broad-spectrum adsorbent tube in series to avoid filter artifacts (Khare et al., 2019). If filter-based
412 methods alone are used to inform organic aerosol emission inventories, then reducing the uncertainty in the
413 relationship between particle emission factor and total CROC will strengthen our confidence in estimating organic
414 aerosol emissions, particularly for lower-emitting technologies. Some CROC/OM ratios derived for this work are
415 between 0.85 and 1.15, indicating a limited role for partitioning bias during source testing in those cases, but many
416 are greater than 1.30, especially the lower-emitting sources. Lastly, more research is needed to determine the extent
417 to which NMOG measurements capture IVOCs (quantified by the IVOC/NMOG or IVOC/GROC ratios). These
418 parameters are especially important to understand for older vehicles and equipment which drive historical and
419 contemporary emissions. We recommend that emissions tests specifically measure and report CROC and GROC to
420 facilitate comparison among datasets and implementation in emission models. Currently, these measurements are
421 beyond the scope of typical regulatory requirements, and future progress requires research beyond regulatory methods.

422 **ASSOCIATED CONTENT**

423 The Supporting Information is available free of charge at

424 Supporting Information 1 (SI-1): Word Document

425 Supporting Information 2 (SI-2): Excel Sheet with Tables

426 The CMAQ model source code used is available via Zenodo (<https://doi.org/10.5281/zenodo.7869142>). The functions
427 to estimate OA and O₃ potential are available at <https://github.com/USEPA/CRAACMM>.

428 **ACKNOWLEDGMENT**

429 The authors gratefully acknowledge contributions from U.S. EPA staff including Kristen Foley and George Pouliot
430 who for emissions inputs and Chad Bailey, Michael Hays, and Sergey Napelenok for internal technical reviews. We
431 also acknowledge Yunliang Zhao of the California Air Resources Board for valuable insights and consultation.

432 **AUTHOR INFORMATION**

433 ***Corresponding Author:** Benjamin N. Murphy; Address: Center for Environmental Measurement and Modeling,
434 109 TW Alexander Dr., Durham, NC 27709, USA; Email: murphy.ben@epa.gov; Phone: 919-541-2291

435 **Author Contributions**

436 The manuscript was written and revised through contributions of all authors. All authors have given approval to the
437 final version of the manuscript. DS made contributions to the study primarily when employed by US EPA.

438 **DISCLAIMER**

439 *The views expressed in this article are those of the author(s) and do not necessarily represent the views or the policies*
440 *of the U.S. Environmental Protection Agency*

441 **COMPETING INTERESTS.**

442 *Some authors are members of the editorial board of ACP. The peer-review process was guided by an independent*
443 *editor, and the authors have also no other competing interests to declare.*

444 **REFERENCES**

- 445 Ahmadov, R., McKeen, S. A., Robinson, A. L., Bahreini, R., Middlebrook, A. M., de Gouw, J. A., Meagher, J.,
446 Hsie, E. Y., Edgerton, E., Shaw, S., and Trainer, M.: A volatility basis set model for summertime secondary
447 organic aerosols over the eastern united states in 2006, *J Geophys Res-Atmos*, 117, 10.1029/2011jd016831,
448 2012.
- 449 Appel, K. W., Bash, J. O., Fahey, K. M., Foley, K. M., Gilliam, R. C., Hogrefe, C., Hutzell, W. T., Kang, D.,
450 Mathur, R., Murphy, B. N., Napelenok, S. L., Nolte, C. G., Pleim, J. E., Pouliot, G. A., Pye, H. O. T., Ran,
451 L., Roselle, S. J., Sarwar, G., Schwede, D. B., Sidi, F. I., Spero, T. L., and Wong, D. C.: The community
452 multiscale air quality (cmaq) model versions 5.3 and 5.3.1: System updates and evaluation, *Geosci Model*
453 *Dev*, 14, 2867-2897, 10.5194/gmd-14-2867-2021, 2021.
- 454 Bergström, R., Denier Van Der Gon, H., Prévôt, A. S., Yttri, K. E., and Simpson, D.: Modelling of organic aerosols
455 over europe (2002–2007) using a volatility basis set (vbs) framework: Application of different assumptions
456 regarding the formation of secondary organic aerosol, *Atmospheric Chemistry and Physics*, 12, 8499-8527,
457 10.5194/acp-12-8499-2012, 2012.
- 458 Bessagnet, B., Allemand, N., Putaud, J. P., Couvidat, F., Andre, J. M., Simpson, D., Pisoni, E., Murphy, B. N., and
459 Thunis, P.: Emissions of carbonaceous particulate matter and ultrafine particles from vehicles-a scientific
460 review in a cross-cutting context of air pollution and climate change, *Appl Sci (Basel)*, 12, 1-52,
461 10.3390/app12073623, 2022.
- 462 Birch, M. and Cary, R.: Elemental carbon-based method for monitoring occupational exposures to particulate diesel
463 exhaust, *Aerosol Science and Technology*, 25, 221-241, 10.1080/02786829608965393, 1996.
- 464 Chang, X., Zhao, B., Zheng, H. T., Wang, S. X., Cai, S. Y., Guo, F. Q., Gui, P., Huang, G. H., Wu, D., Han, L. C.,
465 Xing, J., Man, H. Y., Hu, R. L., Liang, C. R., Xu, Q. C., Qiu, X. H., Ding, D., Liu, K. Y., Han, R.,
466 Robinson, A. L., and Donahue, N. M.: Full-volatility emission framework corrects missing and
467 underestimated secondary organic aerosol sources, *One Earth*, 5, 403-412, 10.1016/j.oneear.2022.03.015,
468 2022.
- 469 Chow, J. C., Watson, J. G., Pritchett, L. C., Pierson, W. R., Frazier, C. A., and Purcell, R. G.: The dri thermal/optical
470 reflectance carbon analysis system: Description, evaluation and applications in us air quality studies,
471 *Atmospheric Environment. Part A. General Topics*, 27, 1185-1201, 10.1016/0960-1686(93)90245-T, 1993.
- 472 Donahue, N. M., Robinson, A. L., and Pandis, S. N.: Atmospheric organic particulate matter: From smoke to
473 secondary organic aerosol, *Atmospheric Environment*, 43, 94-106, 10.1016/j.atmosenv.2008.09.055, 2009.
- 474 Drozd, G. T., Zhao, Y., Saliba, G., Frodin, B., Maddox, C., Oliver Chang, M.-C., Maldonado, H., Sardar, S., Weber,
475 R. J., and Robinson, A. L.: Detailed speciation of intermediate volatility and semivolatile organic
476 compound emissions from gasoline vehicles: Effects of cold-starts and implications for secondary organic
477 aerosol formation, *Environmental science & technology*, 53, 1706-1714, 10.1021/acs.est.8b05600, 2018.
- 478 FAA: Aviation environmental design tool (aedt) version 3e, U.S Department of Transportation <https://aedt.faa.gov/>,
479 2022.
- 480 Foley, K. M., Pouliot, G. A., Eyth, A., Aldridge, M. F., Allen, C., Appel, K. W., Bash, J. O., Beardsley, M., Beidler,
481 J., and Choi, D.: 2002-2017 anthropogenic emissions data for air quality modeling over the united states,
482 *Data in Brief*, 109022, 10.1016/j.dib.2023.109022, 2023.
- 483 Gentner, D. R., Harley, R. A., Miller, A. M., and Goldstein, A. H.: Diurnal and seasonal variability of gasoline-
484 related volatile organic compound emissions in riverside, california, *Environmental science & technology*,
485 43, 4247-4252, 10.1021/es9006228, 2009.
- 486 Gentner, D. R., Isaacman, G., Worton, D. R., Chan, A. W., Dallmann, T. R., Davis, L., Liu, S., Day, D. A., Russell,
487 L. M., Wilson, K. R., Weber, R., Guha, A., Harley, R. A., and Goldstein, A. H.: Elucidating secondary

488 organic aerosol from diesel and gasoline vehicles through detailed characterization of organic carbon
 489 emissions, *Proc Natl Acad Sci U S A*, 109, 18318-18323, 10.1073/pnas.1212272109, 2012.
 490 Gentner, D. R., Jathar, S. H., Gordon, T. D., Bahreini, R., Day, D. A., El Haddad, I., Hayes, P. L., Pieber, S. M.,
 491 Platt, S. M., de Gouw, J., Goldstein, A. H., Harley, R. A., Jimenez, J. L., Prevot, A. S., and Robinson, A.
 492 L.: Review of urban secondary organic aerosol formation from gasoline and diesel motor vehicle
 493 emissions, *Environ Sci Technol*, 51, 1074-1093, 10.1021/acs.est.6b04509, 2017.
 494 Heald, C. L. and Kroll, J. H.: The fuel of atmospheric chemistry: Toward a complete description of reactive organic
 495 carbon, *Sci Adv*, 6, eaay8967, 10.1126/sciadv.aay8967, 2020.
 496 Huang, C., Hu, Q., Li, Y., Tian, J., Ma, Y., Zhao, Y., Feng, J., An, J., Qiao, L., Wang, H., Jing, S., Huang, D., Lou,
 497 S., Zhou, M., Zhu, S., Tao, S., and Li, L.: Intermediate volatility organic compound emissions from a large
 498 cargo vessel operated under real-world conditions, *Environ Sci Technol*, 52, 12934-12942,
 499 10.1021/acs.est.8b04418, 2018.
 500 Humes, M. B., Wang, M., Kim, S., Machesky, J. E., Gentner, D. R., Robinson, A. L., Donahue, N. M., and Presto,
 501 A. A.: Limited secondary organic aerosol production from acyclic oxygenated volatile chemical products,
 502 *Environmental Science & Technology*, 56, 4806-4815, 10.1021/acs.est.1c07354, 2022.
 503 Jathar, S. H., Woody, M., Pye, H. O. T., Baker, K. R., and Robinson, A. L.: Chemical transport model simulations
 504 of organic aerosol in southern california: Model evaluation and gasoline and diesel source contributions,
 505 *Atmos Chem Phys*, 17, 4305-4318, 10.5194/acp-17-4305-2017, 2017a.
 506 Jathar, S. H., Friedman, B., Galang, A. A., Link, M. F., Brophy, P., Volckens, J., Eluri, S., and Farmer, D. K.:
 507 Linking load, fuel, and emission controls to photochemical production of secondary organic aerosol from a
 508 diesel engine, *Environ Sci Technol*, 51, 1377-1386, 10.1021/acs.est.6b04602, 2017b.
 509 Jathar, S. H., Sharma, N., Galang, A., Vanderheyden, C., Takhar, M., Chan, A. W. H., Pierce, J. R., and Volckens,
 510 J.: Measuring and modeling the primary organic aerosol volatility from a modern non-road diesel engine,
 511 *Atmospheric Environment*, 223, 117221, 10.1016/j.atmosenv.2019.117221, 2020.
 512 Khare, P., Marcotte, A., Sheu, R., Walsh, A. N., Ditto, J. C., and Gentner, D. R.: Advances in offline approaches for
 513 trace measurements of complex organic compound mixtures via soft ionization and high-resolution tandem
 514 mass spectrometry, *Journal of Chromatography A*, 1598, 163-174, 10.1016/j.chroma.2018.09.014, 2019.
 515 Kishan, S., Burnette, A., FUNcher, S., Sabisch, M., Crews, E., Snow, R., Zmud, M., Santos, R., Bricka, S., Fujita, E.,
 516 Campbell, D., and Arnott, P.: Kansas city pm characterization study final report, 2006.
 517 Koo, B., Knipping, E., and Yarwood, G.: 1.5-dimensional volatility basis set approach for modeling organic aerosol
 518 in camx and cmaq, *Atmospheric Environment*, 95, 158-164, 10.1016/j.atmosenv.2014.06.031, 2014.
 519 Lim, Y. B. and Ziemann, P. J.: Chemistry of secondary organic aerosol formation from oh radical-initiated reactions
 520 of linear, branched, and cyclic alkanes in the presence of no x, *Aerosol Science and Technology*, 43, 604-
 521 619, 10.1080/02786820902802567, 2009.
 522 Lipsky, E. M. and Robinson, A. L.: Effects of dilution on fine particle mass and partitioning of semivolatile organics
 523 in diesel exhaust and wood smoke, *Environ Sci Technol*, 40, 155-162, 10.1021/es050319p, 2006.
 524 Lu, Q., Murphy, B. N., Qin, M., Adams, P. J., Zhao, Y., Pye, H. O. T., Efstathiou, C., Allen, C., and Robinson, A.
 525 L.: Simulation of organic aerosol formation during the calnex study: Updated mobile emissions and
 526 secondary organic aerosol parameterization for intermediate-volatility organic compounds, *Atmos Chem
 527 Phys*, 20, 4313-4332, 10.5194/acp-20-4313-2020, 2020.
 528 Lu, Q. Y., Zhao, Y. L., and Robinson, A. L.: Comprehensive organic emission profiles for gasoline, diesel, and gas-
 529 turbine engines including intermediate and semi-volatile organic compound emissions, *Atmospheric
 530 Chemistry and Physics*, 18, 17637-17654, 10.5194/acp-18-17637-2018, 2018.
 531 Lurmann, F., Avol, E., and Gilliland, F.: Emissions reduction policies and recent trends in southern california's
 532 ambient air quality, *J Air Waste Manag Assoc*, 65, 324-335, 10.1080/10962247.2014.991856, 2015.
 533 Manavi, S. E. and Pandis, S. N.: A lumped species approach for the simulation of secondary organic aerosol
 534 production from intermediate volatility organic compounds (ivocs): Application to road transport in
 535 pmcamx-iv (v1. 0), *Geoscientific Model Development Discussions*, 1-35, 10.5194/gmd-2022-90, 2022.
 536 May, A. A., Presto, A. A., Hennigan, C. J., Nguyen, N. T., Gordon, T. D., and Robinson, A. L.: Gas-particle
 537 partitioning of primary organic aerosol emissions: (2) diesel vehicles, *Environ Sci Technol*, 47, 8288-8296,
 538 10.1021/es400782j, 2013a.
 539 May, A. A., Presto, A. A., Hennigan, C. J., Nguyen, N. T., Gordon, T. D., and Robinson, A. L.: Gas-particle
 540 partitioning of primary organic aerosol emissions: (1) gasoline vehicle exhaust, *Atmospheric Environment*,
 541 77, 128-139, 10.1016/j.atmosenv.2013.04.060, 2013b.
 542 May, A. A., Nguyen, N. T., Presto, A. A., Gordon, T. D., Lipsky, E. M., Karve, M., Gutierrez, A., Robertson, W. H.,
 543 Zhang, M., Brandow, C., Chang, O., Chen, S. Y., Cicero-Fernandez, P., Dinkins, L., Fuentes, M., Huang,

544 S. M., Ling, R., Long, J., Maddox, C., Massetti, J., McCauley, E., Miguel, A., Na, K., Ong, R., Pang, Y. B.,
545 Rieger, P., Sax, T., Truong, T., Vo, T., Chattopadhyay, S., Maldonado, H., Maricq, M. M., and Robinson,
546 A. L.: Gas- and particle-phase primary emissions from in-use, on-road gasoline and diesel vehicles,
547 *Atmospheric Environment*, 88, 247-260, 10.1016/j.atmosenv.2014.01.046, 2014.

548 Morino, Y., Chatani, S., Fujitani, Y., Tanabe, K., Murphy, B. N., Jathar, S. H., Takahashi, K., Sato, K., Kumagai,
549 K., and Saito, S.: Emissions of condensable organic aerosols from stationary combustion sources over
550 Japan, *Atmospheric Environment*, 289, 119319, 10.1016/j.atmosenv.2022.119319, 2022.

551 Murphy, B. N. and Pandis, S. N.: Simulating the formation of semivolatile primary and secondary organic aerosol in
552 a regional chemical transport model, *Environ Sci Technol*, 43, 4722-4728, 10.1021/es803168a, 2009.

553 Murphy, B. N., Donahue, N. M., Robinson, A. L., and Pandis, S. N.: A naming convention for atmospheric organic
554 aerosol, *Atmospheric Chemistry and Physics*, 14, 5825-5839, 10.5194/acp-14-5825-2014, 2014.

555 Murphy, B. N., Woody, M. C., Jimenez, J. L., Carlton, A. M. G., Hayes, P. L., Liu, S., Ng, N. L., Russell, L. M.,
556 Setyan, A., Xu, L., Young, J., Zaveri, R. A., Zhang, Q., and Pye, H. O. T.: Semivolatile poa and
557 parameterized total combustion soa in cmaq5.2: Impacts on source strength and partitioning, *Atmos Chem
558 Phys*, 17, 11107-11133, 10.5194/acp-17-11107-2017, 2017.

559 Pennington, E. A., Seltzer, K. M., Murphy, B. N., Qin, M., Seinfeld, J. H., and Pye, H. O.: Modeling secondary
560 organic aerosol formation from volatile chemical products, *Atmospheric chemistry and physics*, 21, 18247-
561 18261, 10.5194/acp-21-18247-2021, 2021.

562 Pye, H. O. T., Appel, K. W., Seltzer, K. M., Ward-Caviness, C. K., and Murphy, B. N.: Human-health impacts of
563 controlling secondary air pollution precursors, *Environ Sci Technol Lett*, 9, 96-101,
564 10.1021/acs.estlett.1c00798, 2022a.

565 Pye, H. O. T., Place, B. K., Murphy, B. N., Seltzer, K. M., and D'Ambro, E. L.: Linking gas, particulate, and toxic
566 endpoints to air emissions in the community regional atmospheric chemistry multiphase mechanism
567 (cracmm) version 1.0 *Atmospheric Chemistry and Physics*, 2022b.

568 Pye, H. O. T., Ward-Caviness, C. K., Murphy, B. N., Appel, K. W., and Seltzer, K. M.: Secondary organic aerosol
569 association with cardiorespiratory disease mortality in the United States, *Nat Commun*, 12, 7215,
570 10.1038/s41467-021-27484-1, 2021.

571 Reff, A., Bhawe, P. V., Simon, H., Pace, T. G., Pouliot, G. A., Mobley, J. D., and Houyoux, M.: Emissions inventory
572 of pm_{2.5} trace elements across the United States, *Environ Sci Technol*, 43, 5790-5796, 10.1021/es802930x,
573 2009.

574 Robinson, A. L., Grieshop, A. P., Donahue, N. M., and Hunt, S. W.: Updating the conceptual model for fine particle
575 mass emissions from combustion systems Allen I. Robinson, *Journal of the Air & Waste Management
576 Association*, 60, 1204-1222, 10.3155/1047-3289.60.10.1204, 2010.

577 Robinson, A. L., Donahue, N. M., Shrivastava, M. K., Weitkamp, E. A., Sage, A. M., Grieshop, A. P., Lane, T. E.,
578 Pierce, J. R., and Pandis, S. N.: Rethinking organic aerosols: Semivolatile emissions and photochemical
579 aging, *Science*, 315, 1259-1262, 10.1126/science.1133061, 2007.

580 Safieddine, S. A., Heald, C. L., and Henderson, B. H.: The global nonmethane reactive organic carbon budget: A
581 modeling perspective, *Geophysical Research Letters*, 44, 3897-3906, 10.1002/2017gl072602, 2017.

582 Sarica, T., Sartelet, K., Roustan, Y., Kim, Y., Lugon, L., Marques, B., D'Anna, B., Chaillou, C., and Larrieu, C.:
583 Sensitivity of pollutant concentrations in urban streets to asphalt and traffic-related emissions,
584 *Environmental Pollution*, 121955, 10.1016/j.envpol.2023.121955, 2023.

585 Seltzer, K. M., Pennington, E., Rao, V., Murphy, B. N., Strum, M., Isaacs, K. K., and Pye, H. O. T.: Reactive
586 organic carbon emissions from volatile chemical products, *Atmos Chem Phys*, 21, 5079-5100,
587 10.5194/acp-21-5079-2021, 2021.

588 Shrivastava, M., Fast, J., Easter, R., Gustafson, W. I., Zaveri, R. A., Jimenez, J. L., Saide, P., and Hodzic, A.:
589 Modeling organic aerosols in a megacity: Comparison of simple and complex representations of the
590 volatility basis set approach, *Atmospheric Chemistry and Physics*, 11, 6639-6662, 10.5194/acp-11-6639-
591 2011, 2011.

592 Simon, H., Bhawe, P. V., Swall, J. L., Frank, N. H., and Malm, W. C.: Determining the spatial and seasonal
593 variability in om/oc ratios across the US using multiple regression, *Atmospheric Chemistry and Physics*, 11,
594 2933-2949, 10.5194/acp-11-2933-2011, 2011.

595 Tessum, C. W., Paoletta, D. A., Chambliss, S. E., Apte, J. S., Hill, J. D., and Marshall, J. D.: Pm_{2.5} pollutants
596 disproportionately and systemically affect people of color in the United States, *Sci Adv*, 7, eabf4491,
597 10.1126/sciadv.abf4491, 2021.

598 Tkacik, D. S., Presto, A. A., Donahue, N. M., and Robinson, A. L.: Secondary organic aerosol formation from
599 intermediate-volatility organic compounds: Cyclic, linear, and branched alkanes, *Environ Sci Technol*, 46,
600 8773-8781, 10.1021/es301112c, 2012.

601 Turpin, B. J., Huntzicker, J. J., and Hering, S. V.: Investigation of organic aerosol sampling artifacts in the los-
602 angeles basin, *Atmospheric Environment*, 28, 3061-3071, 10.1016/1352-2310(94)00133-6, 1994.

603 U.S. EPA: Integrated science assessment (isa) for particulate matter (final report, dec 2019), 2019.

604 U.S. EPA: Speciatev5.1, U.S. EPA <https://www.epa.gov/air-emissions-modeling/speciate>, 2020a.

605 U.S. EPA: Motor vehicle emission simulator: Moves3, Office of Transportation and Air Quality, U.S. EPA
606 <https://www.epa.gov/moves>, 2020b.

607 U.S. EPA: Integrated science assessment (isa) for ozone and related photochemical oxidants (final report, apr 2020),
608 2020c.

609 U.S. EPA: Community multiscale air quality (cmaq) model v5.3.2, Office of Research and Development, U.S. EPA
610 <https://github.com/USEPA/CMAQ/tree/5.3.2>, 2021.

611 U.S. EPA: Equates: Epa's air quality time series project, U.S. EPA [dataset], 2022a.

612 U.S. EPA: Technical support document (tsd) preparation of emissions inventories for the 2017 north american
613 emissions modeling platform, 2022b.

614 U.S. EPA: Engine testing procedures. Cfr, part 1065, title 40, 2022c.

615 Winkler, S., Anderson, J., Garza, L., Ruona, W., Vogt, R., and Wallington, T.: Vehicle criteria pollutant (pm, nox,
616 co, hcs) emissions: How low should we go?, *Npj Climate and atmospheric science*, 1, 1-5, 10.1038/s41612-
617 018-0037-5, 2018.

618 Woody, M. C., West, J. J., Jathar, S. H., Robinson, A. L., and Arunachalam, S.: Estimates of non-traditional
619 secondary organic aerosols from aircraft svoc and ivoc emissions using cmaq, *Atmospheric Chemistry and
620 Physics*, 15, 6929-6942, 10.5194/acp-15-6929-2015, 2015.

621 Woody, M. C., Baker, K. R., Hayes, P. L., Jimenez, J. L., Koo, B., and Pye, H. O.: Understanding sources of organic
622 aerosol during calnex-2010 using the cmaq-vbs, *Atmospheric Chemistry and Physics*, 16, 4081-4100,
623 10.5194/acp-16-4081-2016, 2016.

624 Worton, D. R., Isaacman, G., Gentner, D. R., Dallmann, T. R., Chan, A. W., Ruehl, C., Kirchstetter, T. W., Wilson,
625 K. R., Harley, R. A., and Goldstein, A. H.: Lubricating oil dominates primary organic aerosol emissions
626 from motor vehicles, *Environmental science & technology*, 48, 3698-3706, 10.1021/es405375j, 2014.

627 Yee, L., Craven, J., Loza, C., Schilling, K., Ng, N., Canagaratna, M., Ziemann, P., Flagan, R., and Seinfeld, J.:
628 Effect of chemical structure on secondary organic aerosol formation from c 12 alkanes, *Atmospheric
629 Chemistry and Physics*, 13, 11121-11140, 10.5194/acp-13-11121-2013, 2013.

630 Zhang, X., Cappa, C. D., Jathar, S. H., McVay, R. C., Ensberg, J. J., Kleeman, M. J., and Seinfeld, J. H.: Influence
631 of vapor wall loss in laboratory chambers on yields of secondary organic aerosol, *Proceedings of the
632 National Academy of Sciences*, 111, 5802-5807, 10.1073/pnas.1404727111, 2014.

633 Zhao, B., Wang, S., Donahue, N. M., Jathar, S. H., Huang, X., Wu, W., Hao, J., and Robinson, A. L.: Quantifying
634 the effect of organic aerosol aging and intermediate-volatility emissions on regional-scale aerosol pollution
635 in china, *Sci Rep*, 6, 28815, 10.1038/srep28815, 2016a.

636 Zhao, Y., Tkacik, D. S., May, A. A., Donahue, N. M., and Robinson, A. L.: Mobile sources are still an important
637 source of secondary organic aerosol and fine particulate matter in the los angeles region, *Environmental
638 Science & Technology*, 56, 15328-15336, 10.1021/acs.est.2c03317, 2022.

639 Zhao, Y., Nguyen, N. T., Presto, A. A., Hennigan, C. J., May, A. A., and Robinson, A. L.: Intermediate volatility
640 organic compound emissions from on-road diesel vehicles: Chemical composition, emission factors, and
641 estimated secondary organic aerosol production, *Environ Sci Technol*, 49, 11516-11526,
642 10.1021/acs.est.5b02841, 2015.

643 Zhao, Y., Nguyen, N. T., Presto, A. A., Hennigan, C. J., May, A. A., and Robinson, A. L.: Intermediate volatility
644 organic compound emissions from on-road gasoline vehicles and small off-road gasoline engines, *Environ
645 Sci Technol*, 50, 4554-4563, 10.1021/acs.est.5b06247, 2016b.

646 Zhao, Y., Hennigan, C. J., May, A. A., Tkacik, D. S., de Gouw, J. A., Gilman, J. B., Kuster, W. C., Borbon, A., and
647 Robinson, A. L.: Intermediate-volatility organic compounds: A large source of secondary organic aerosol,
648 *Environ Sci Technol*, 48, 13743-13750, 10.1021/es5035188, 2014.

649

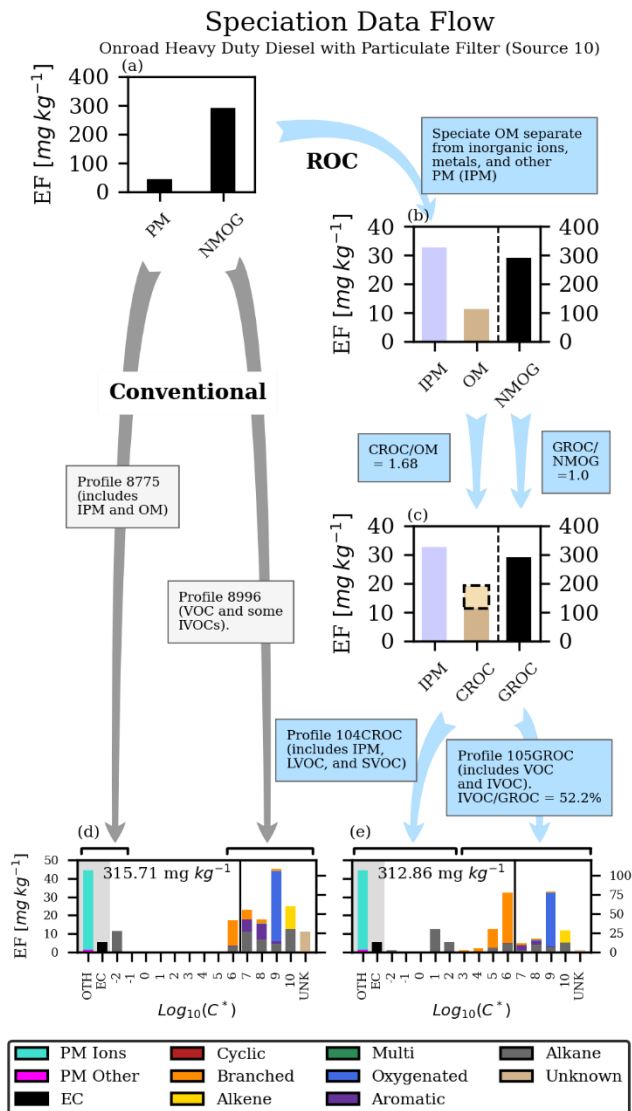
650

651

653 **Table 1.** Definitions of key terms.

| Acronym | Definition |
|----------------|---|
| OM | Organic matter component of primary particle emissions as measured on a filter. |
| NMOG | Non-methane organic gas emissions |
| POA | Primary organic aerosol. Particle-phase emissions after equilibrium is reached with ambient conditions. |
| OA | Particle-phase organic material at ambient conditions. |
| LVOC | Low-volatility organic compounds ($C^* \leq 0.32 \mu\text{g m}^{-3}$). |
| SVOC | Semivolatile organic compounds ($0.32 < C^* \leq 320 \mu\text{g m}^{-3}$). |
| IVOC | Intermediate volatility organic compounds ($320 < C^* \leq 3.2 \times 10^6 \mu\text{g m}^{-3}$). |
| VOC | Volatile organic compounds ($3.2 \times 10^6 \mu\text{g m}^{-3} < C^*$). |
| CROC | Condensable reactive organic carbon: particle- and gas-phase LVOC + SVOC. Carbon and noncarbon mass are included. |
| GROC | Gaseous reactive organic carbon: particle- and gas-phase IVOC + VOC. Carbon and noncarbon mass are included. |
| ROC | Reactive organic carbon – all particle and gas organic compounds mass except methane. Carbon and noncarbon mass are included. |

654
655



656

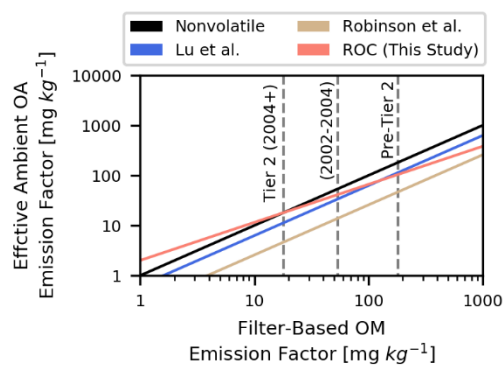
657 **Figure 1.** Depiction of calculation steps for the Conventional and ROC approaches to speciation of PM and NMOG
 658 emissions. Panel (a) shows the reported fuel-based emission factors based on MOVES predictions for 2016. Panel
 659 (b) shows the inorganic ions, metals and other nonorganic matter (IPM) separated from organic matter (OM). The
 660 beige area inside the dashed box in panel (c) indicates emissions that are added in the conversion of OM to CROC to
 661 account for underrepresented SVOCs from the filter measurement. Panels (d) and (e) show the comprehensive
 662 emission factors for the Conventional and ROC approaches, respectively, with data arranged by volatility while
 663 indicating non-organic PM emissions as well. In panels (d) and (e), bars to the left and right of the vertical line at
 664 $\text{Log}_{10}(\text{C}^*) = 6.5$ are quantified by the left and right y axes, respectively. The number within panels (d) and (e)
 665 indicates the total ROC emission factor excluding EC and Other PM for onroad heavy-duty diesel sources. ‘Alkane’
 666 refers to only linear alkanes, while ‘cyclic’ and ‘branched’ are cyclic alkanes and branched alkanes. ‘Multi’

667 indicates multifunctional organics. The bars in the gray shaded regions are not included in the organic volatility
668 distribution but are included in the CROC-compatible SPECIATE profiles (e.g. 104CROC).

669

670

671

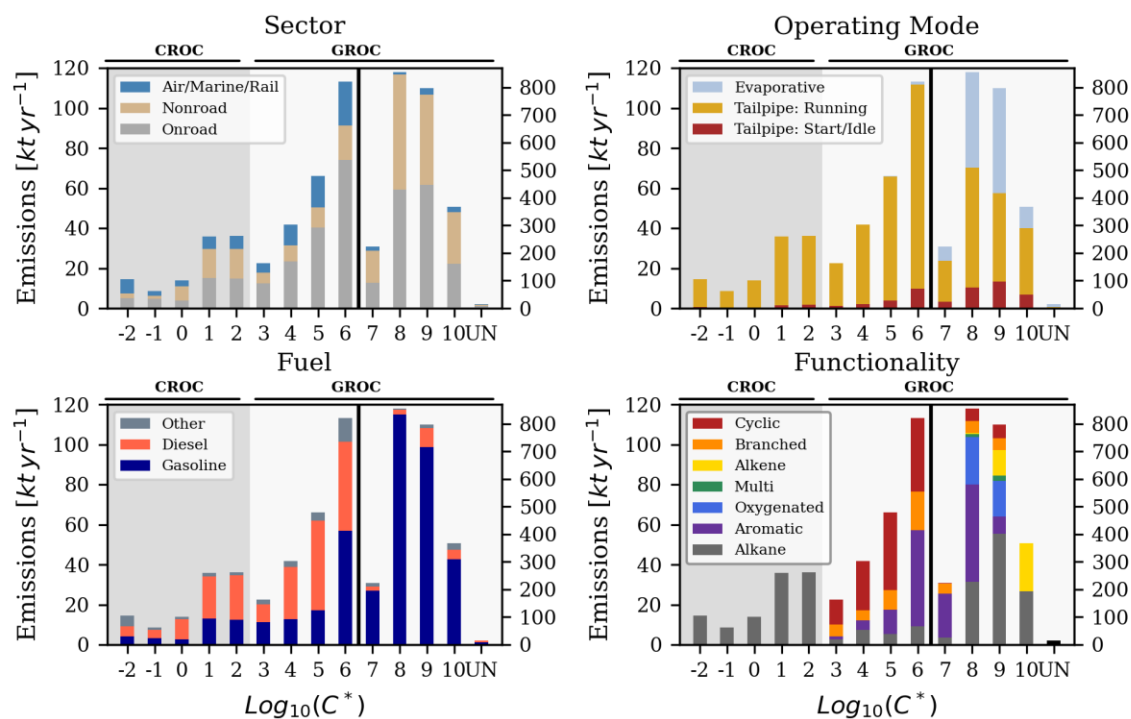


672

673 **Figure 2.** Effective ambient primary organic aerosol emission factor estimated at 298 K and $10 \mu\text{g m}^{-3}$ as a function
674 of the OM emission factor for onroad gasoline-fueled vehicles.

675

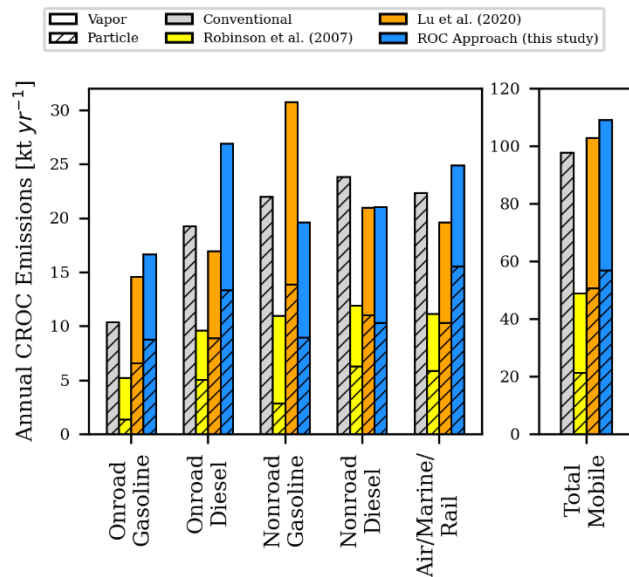
676



677

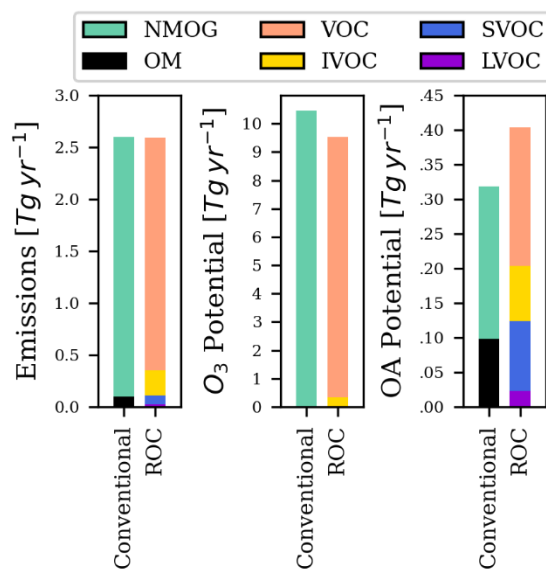
678 **Figure 3.** Volatility-resolved mobile source ROC emissions for the contiguous U.S. during 2016 stratified along
 679 several dimensions including category (top-left), operating mode (top-right), fuel (bottom-left), and chemical
 680 functionality (bottom-right). The ‘multi’ functionality series corresponds to compounds that are both oxygenated and
 681 have double carbon bonds. Bins to the left of the solid black line are quantified by the left y axis and those to the right
 682 by the right y axis. The unknown emissions (UN) are not assigned to a volatility bin and do not contribute to OA or
 683 O_3 formation.

684



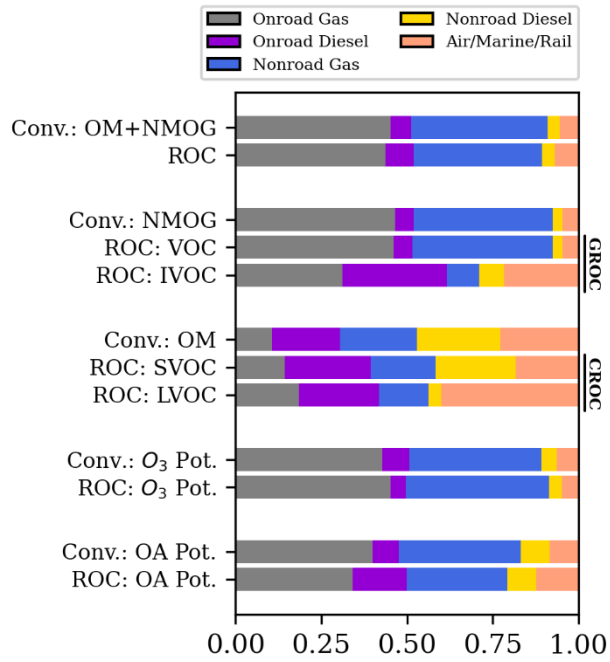
685
 686 **Figure 4.** Bottom-up predictions of 2016 annual mobile CROC (i.e. SVOC, LVOC, and lower volatility compound)
 687 emissions classified by category, model approach, and equilibrium phase distribution. The full height of each bar
 688 corresponds to total CROC emissions. Gas-particle partitioning is calculated for atmospherically relevant conditions
 689 at 298 K and organic aerosol loading of $10 \mu\text{g m}^{-3}$.

690
 691
 692

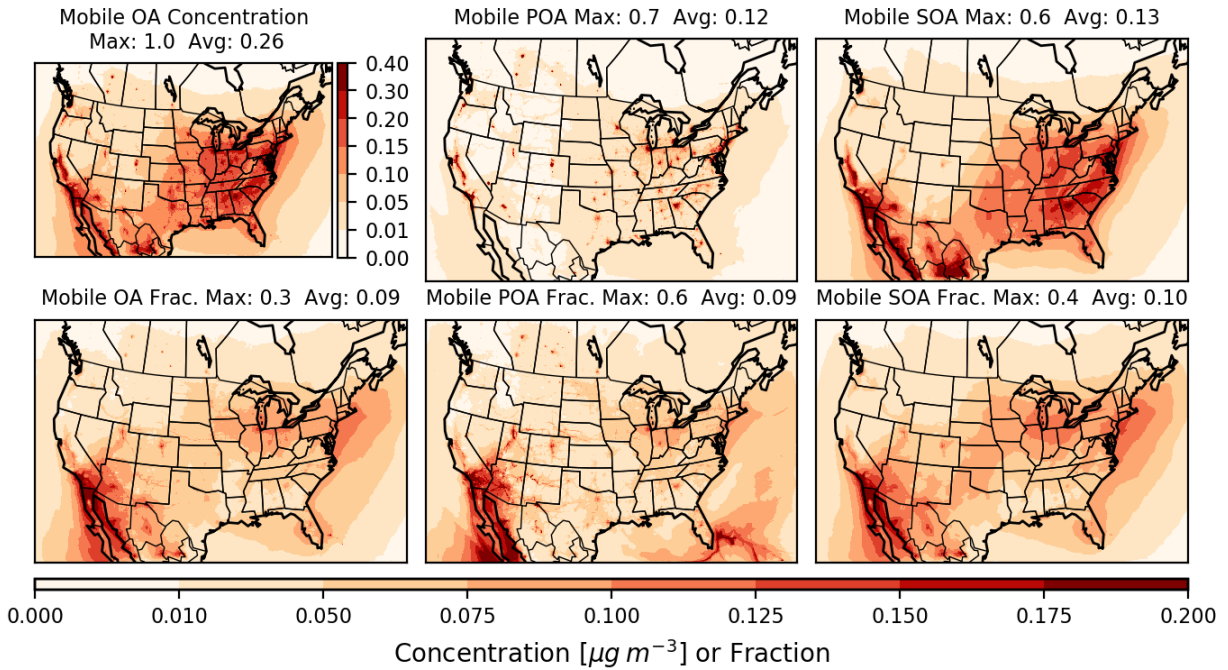


693
 694 **Figure 5.** Total U. S. mobile source emissions for 2016 with aggregate O_3 and OA potential calculated at the species
 695 level.

696

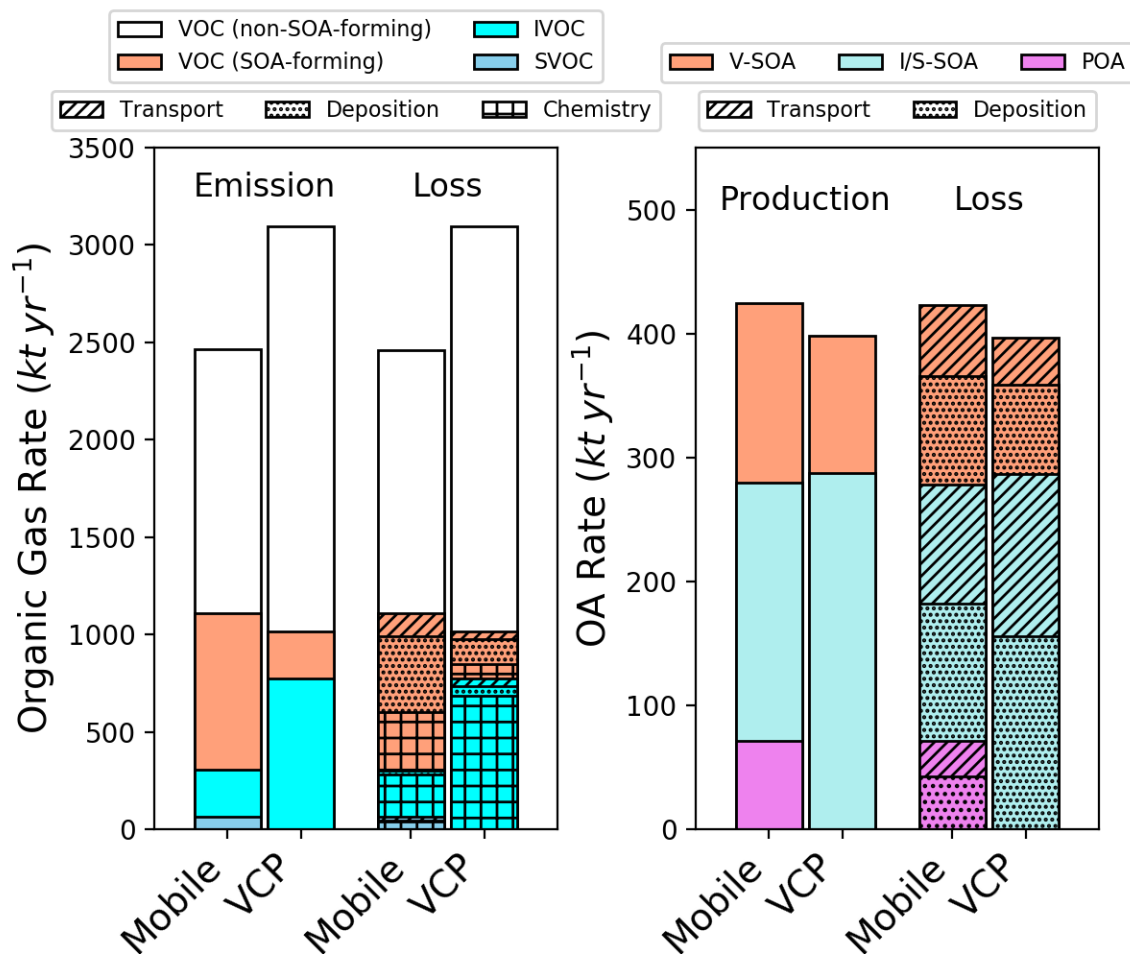


697
 698 **Figure 6.** Mobile sector contributions to ROC classes and derived quantities like O₃ and OA potential. Values are
 699 presented for the Conventional and ROC-based approaches.



700

701 **Figure 7.** Annual average concentration (top row) of total OA (left), POA (center), and SOA (right) from mobile
 702 sources predicted by CMAQ for 2017 with the ROC mobile emission inventory. The fractional contribution of mobile
 703 sources to the total of each pollutant category from all sources are on the bottom row. In all panel subtitles, 'Max'
 704 refers to the spatial maximum of the annual average spatial field, while 'Avg' refers to the population-weighted
 705 average of the annual average spatial field.



706
 707
 708
 709
 710
 711
 712
 713

Figure 8. Domain-wide predicted budget of (left) mobile and volatile chemical product (VCP) gas-phase emissions and loss due to chemistry, deposition, or transport and (right) OA production and losses for 2017. In the left plot, loss terms are only depicted for categories of compounds that lead to organic particle formation.